HHS Public Access

Author manuscript

Proc SPIE Int Soc Opt Eng. Author manuscript; available in PMC 2018 January 22.

Published in final edited form as:

Proc SPIE Int Soc Opt Eng. 2016 ; 9785: . doi:10.1117/12.2216898.

Assessing vertebral fracture risk on volumetric quantitative computed tomography by geometric characterization of trabecular bone structure

Walter A. Checefsky[1], **Anas Z. Abidin**[2], **Mahesh B. Nagarajan**[2], **Jan S. Bauer**[4], **Thomas Baum**[4], and **Axel Wismüller**[1,2,3]

[1]Department of Electrical and Computer Engineering, University of Rochester, New York, United States

[2]Departments of Imaging Sciences and Biomedical Engineering, University of Rochester, New York, United States

[3]Faculty of Medicine and Institute of Clinical Radiology, Ludwig Maximilian University, Munich, Germany

[4]Institute for Diagnostic and Interventional Radiology, Technical University of Munich, Germany

Abstract

The current clinical standard for measuring Bone Mineral Density (BMD) is dual X-ray absorptiometry, however more recently BMD derived from volumetric quantitative computed tomography has been shown to demonstrate a high association with spinal fracture susceptibility. In this study, we propose a method of fracture risk assessment using structural properties of trabecular bone in spinal vertebrae. Experimental data was acquired via axial multi-detector CT (MDCT) from 12 spinal vertebrae specimens using a whole-body 256-row CT scanner with a dedicated calibration phantom. Common image processing methods were used to annotate the trabecular compartment in the vertebral slices creating a circular region of interest (ROI) that excluded cortical bone for each slice. The pixels inside the ROI were converted to values indicative of BMD. High dimensional geometrical features were derived using the scaling index method (SIM) at different radii and scaling factors (SF). The mean BMD values within the ROI were then extracted and used in conjunction with a support vector machine to predict the failure load of the specimens. Prediction performance was measured using the root-mean-square error (RMSE) metric and determined that SIM combined with mean BMD features (RMSE = 0.82 ± 0.37) outperformed MDCT-measured mean BMD (RMSE = 1.11 ± 0.33) ($p < 10^{-4}$). These results demonstrate that biomechanical strength prediction in vertebrae can be significantly improved through the use of SIM-derived texture features from trabecular bone.

Keywords

spinal vertebrae; trabecular bone; biomechanical strength prediction; multi-detector computed tomography; bone mineral density; Scaling Index Method (SIM); support vector regression

This work is not being and has not been submitted for publication or presentation elsewhere.

1. MOTIVATION/PURPOSE

Osteoporosis, one of the most common age-related diseases among elderly people, often leads to fractures which increases the mortality rate and lowers the quality of life. Studies predict that the number of people at risk for osteoporotic fractures worldwide will reach over 6 million by 2050 [1]. Due to the large demographic affected and the current rates of aging in our population, osteoporosis is becoming a significant health problem. The diagnosis and treatment of osteoporosis creates a substantial financial burden [7]. Accurate prediction of osteoporotic fracture risk can be of significant clinical benefit when assessing and managing osteoporosis. Although reduced bone mineral density (BMD) derived from dual X-ray absorptiometry (DXA) is considered a clinical standard for fracture prediction, it has been shown to be susceptible to interference from cortical shells, surrounding tissue and fat. A more thorough characterization can be provided using volumetric quantitative computed tomography (QCT). In this study we demonstrate that using image-based features characterizing the trabecular bone structure, can aid in diagnosing and monitoring osteoporotic bone changes [2–4]. This work is embedded in our group's endeavor to expedite 'big data' analysis in biomedical imaging by means of advanced pattern recognition and machine learning methods for computational radiology and radiomics, e.g. [9–33].

Our study focuses on characterization of trabecular bone structure for the purpose of fracture risk assessment. Correlations between BMD and spinal fracture status have been shown in studies with volumetric QCT. However, while BMD has been a key clinical factor for fracture risk estimation, it does not completely account for individual fracture risk since it does not provide a complete description of bone quality. Here, Scaling index method (SIM)-derived measures are used for multidimensional trabecular bone characterization. Such features are then used as inputs for supervised learning algorithms to construct models for fracture load prediction. The goal is to evaluate whether SIM-derived descriptors of trabecular bone structure can improve bone strength prediction.

2. DATA

2.1 Specimens

The study was designed to biomechanically test spinal segments with intact ligaments, intervertebral discs and posterior elements. Twelve patient specimens were selected, each including 3-segment spinal units. The donors had dedicated their body for educational and research purposes to the local Institute of Anatomy (Technical University of Munich), in compliance with local institutional and legislative requirements. Donors with a history of pathological bone changes other than osteoporosis (such as bone metastases, hematological or metabolic bone disorders) were excluded. The surrounding muscle and fat tissue was completely removed spinal segments. Then, half of the upper and lower vertebra of the spinal segment units was removed with a band saw to create functional spinal segment units with intact ligaments, inter-vertebral discs, and posterior elements. For the purpose of conservation, all functional spinal segment units were stored in formalin solution during the study and degassed at least 24 h before imaging to prevent air artifacts. The functional spinal segment units were sealed in vacuum plastic bags during imaging.

2.2 Imaging with Multi-detector Computed Tomography (MDCT)

Images were acquired using a whole-body 256-row CT scanner (iCT, Philips Medical Care, Best, The Netherlands). A tube voltage of 120 kVp and a tube load of 585 mAs was used to create an image matrix of 1024 × 1024 pixels and a field view of 150 mm. Transverse sections were reconstructed using a high-resolution bone kernel (YE). The interpolated voxel size was 146 × 146 × 300 μm^3 and the real spatial resolution, as determined at q50 of the modulation-transfer-function was 250 × 250 × 600 μm^3. A dedicated calibration phantom (Mindways Osteoporosis Phantom, San Francisco, CA, USA) was placed in the scanner mat beneath the functional spinal units as seen in Figure 1. The reference phantom was used to derive the calcium hydroxyapatite values in BMD (mg/cm^3).

2.3 Image Processing and Volume of Interest (VOI) Selection

The central vertebra of each specimen was used for VOI insertion. For each slice the outer surface of the cortical shell of the spinal segment was isolated automatically based on attenuation differences between cortical and trabecular bone in each image. In a small percentage of specimens, the segmentation mask was improperly calculated by errors induced by high-grade focal bone loss or penetration of adjacent anatomical features. These features include blood vessels and excess tissue remaining after the segments were removed from the donor patients. One of two radiologists performed the manual correction of the segmentation if errors occurred.

2.4 BMD Calculations

Voxel attenuations (Hounsfield Units or HU) on MDCT images were converted to values indicative of BMD using a reference calibration phantom (as seen in Fig 1). The image voxel intensities were converted from HU to BMD units using the following equation as previously outlined in [7]:

$$BMD = \frac{HA_{\mathrm{E}} - HA_{\mathrm{A}}}{HU_{\mathrm{E}} - HU_{\mathrm{A}}} * (HU_{\mathrm{voxel}} - HU_{\mathrm{A}}) \quad (1)$$

The numerator values represent the bone and water densities of the calibration phantoms (E and A), respectively, and HU_E and HU_A are the voxel attenuation values in HU of the corresponding locations of the phantom in the acquired images. HU_{voxel} is the voxel value corresponding to the voxel to be converted to *BMD*.

2.5 Biomechanical Testing

The half-dissected upper and lower vertebrae of the functional spinal segment units were embedded in resin (Rencast Isocyanat and Polyol, Huntsman Group, Bad Säckingen, Germany) up to 2 mm above, respectively, below their vertebral endplates. The fixation was performed with parallel alignment of the upper and lower endplate of middle vertebra with the outer surface of the resin chock to guarantee strict axial loading conditions of the middle vertebra during the uniaxial biomechanical test. After embedding, the functional spinal segment units were fixed in a mechanical testing system (Wolpert Werkstoffprüfmaschinen AG, Schaffhausen, Switzerland). Ten pre-conditioning cycles with uniaxial tension–

compression up to a load between 10 and 400 N with a rate of 5 mm/min was applied. Then a monotonic, uniaxial compression was performed at the same rate. The load–displacement curve was recorded and vertebral failure load was defined as the first peak of the load–displacement curve with a subsequent drop of >10 %. Further details regarding the processes performed to acquire the actual failure load measurements can be seen in [8].

3. METHODS

3.1 BMD Features

The BMD distribution within each VOI was represented by its mean distribution. The measure of BMD on MDCT, using the conversions as shown above, has been shown to be highly correlated to conventional DXA-derived mean BMD values [3].

3.2 Scaling Index Method (SIM) Features

The SIM is a geometrical feature extraction technique proposed by Jamitzky et al. [9]. These can be used to characterize the structural properties of the bone based on its microarchitecture. Briefly, we consider N pixels in a VOI represented by a four-dimensional vector $\mathbf{u}_i = (x_i, y_i, z_i, g_i)$, $i = \{1, \ldots, N\}$, where x_i, y_i and z_i are the geometric coordinates and g_i is the gray-level intensity of the ith pixel, i.e., $g_i = g(x_i, y_i, z_i)$. A local scaling property index α is calculated for each vector $\mathbf{u}_i$ as

$$\alpha(\mathbf{u}_i, R) = \frac{2\sum_{j=1}^{N}(d_{ij}/R)^2 \exp[-(d_{ij}/R)^2]}{\sum_{j=1}^{N}\exp[-(\mathrm{d}_{ij}/\mathrm{R})^2]},$$

where $d_{ij} = \|\mathbf{u}_i, \mathbf{u}_j\|$ is the Euclidean distance between the ith and j^{th} four-dimensional vector and R defines the width of the Gaussian centered on the ith vector. The weighting of geometric and gray-level intensity values for each four-dimensional vector is specified by a scaling factor (SF), which can be optimized for best feature representation. The scaling factors SF = {0.01, 0.1, 1, 10, 100, 200} were applied to the geometric coordinates. Indices α were then calculated for each SF and for the set of radii $R = \{1, 2, 3\}$. The alpha values extracted were distributed evenly into 19 quantiles, which serve as the 19-dimensional feature vector that characterizes each specimen.

3.3 Function Approximation

After geometrical feature computation of trabecular bone, the ability to predict the biomechanical strength, as determined by the failure load according to section 2.5, was evaluated. Machine learning algorithms, namely multiple regression and support vector regression with a linear kernel, were used for the function approximation.

3.4 Prediction Performance

Iteratively, a cross-validation scheme using randomly selected training set of VOIs (70%) was used to approximate the target function, i.e., the failure load. The resulting model was then used to predict the failure load of the remaining independent test set. The independent

test set allowed for unbiased testing of the performance of the bone strength prediction model as calculated by the regression model. The average residual error between the predicted failure load FL_{pred} and the true failure load FL_{true} for the VOIs in this test set T_i, $i = 1,..., N_{iter}$ was measured by the root-mean-square error (RMSE)

$$\mathrm{RMSE}_{\mathrm{T}i} = \sqrt{\langle (\mathrm{FL}_{\mathrm{pred}} - \mathrm{FL}_{\mathrm{true}})^2 \rangle \mathrm{T}_i}.$$

This calculation was repeated iteratively $N_{iter} = 50$ times using randomly chosen train and test sets resulting in a RMSE distribution for each bone feature. A Wilcoxon Signed-Rank Test was used to compare the RMSE distributions and determine statistical significance in performance prediction.

The image processing, feature extraction, machine learning function approximation, evaluation of performance and significance testing were conducted in MATLAB, version R2014a (MathWorks, Natick, MA).

4. RESULTS

The results from evaluation of different machine learning techniques are shown in Figure 2. This study was interested in the relationship between overall prediction performance and the model based on different scaling factors and radius *R.* Different sets of scaling factors and radius values were chosen and the results can be compared between prediction model types. The best feature performance was obtained for SF = 200 and R = 1 when combined with mean BMD features (RMSE = 0.82 ± 0.37). The geometric features outperformed MDCT-measured mean BMD (RMSE = 1.11 ± 0.33) ($p < 10^{-4}$).

5. NEW AND BREAKTHROUGH WORK

BMD measurements derived from MDCT or DXA do not account for a complete characterization of trabecular bone with regard to the micro-architecture, which could limit the accuracy of BMD in predicting bone strength. Here, we demonstrate that SIM features in conjunction with machine learning can be used for accurate prediction of vertebral body fracture load. Advanced characterization of trabecular bone as described in this study may contribute to an improved diagnosis of osteoporosis-related fractures.

This study proposes an automated approach to predict biomechanical strength of spine specimens through the use of BMD analysis in combination with non-linear geometric feature extraction and machine learning techniques. The results suggest that SIM derived properties (radius and scaling factors) are ideal for the application of machine learning models to failure load prediction in osteoporotic bone for diagnosis and monitoring purposes in spinal segments. Furthermore, it can be shown that support vector regression analyses outperform the conventional multiple regression model techniques. Such non-invasive methods for extracting accurate predictors from spinal segments makes this method attractive for use as biomarkers with the task of predicting and monitoring progression of osteoporosis in the spine. We note the certain limitations with this experimental study. The small sample size used reduces the statistical power of the analyses. The spine segments

used in the study were not scanned *in situ* and therefore only represent the soft tissue environment through the use of a water bath. The fact that the specimens were extracted from formalin-fixed cadavers may have affected the biomechanical properties of the segments.

6. CONCLUSION

In conclusion, the results presented in this study show that SIM-derived geometrical features, which characterize trabecular bone microarchitecture, could significantly improve the prediction of biomechanical strength of spinal vertebrae when compared to conventional methods. We hypothesize that our approach can contribute to the development of imaging biomarkers for improved clinical diagnosis and management of osteoporosis. With these biomarkers, disease progression may be tracked and patient response to therapeutic intervention can be monitored. Trabecular structure using high-resolution MDCT is not currently optimal for osteoporosis diagnostics and therapy monitoring due to the high levels of radiation that the patients experience during the image acquisition process. In the future, modalities of image acquisition will need to be implemented before larger controlled trials can be attempted in a clinical setting.

Acknowledgments

This research was funded in part by the National Institute of Health (NIH) Award R01-DA-034977, the Harry W. Fischer Award of the University of Rochester, the Clinical and Translational Science Award 5-28527 within the Upstate New York Translational Research Network (UNYTRN) of the Clinical and Translational Science Institute (CTSI), University of Rochester, by the Center for Emerging and Innovative Sciences (CEIS), a NYSTAR-designated Center for Advanced Technology and by the Deutsche Forschungsgemeinschaft (DFG BA 4085/2-1 (to J.S.B.) and BA 4906/1-1 (to T.B.)). The content is solely the responsibility of the authors and does not necessarily represent the official views of the National Institute of Health. This work was conducted as a Practice Quality Improvement (PQI) project related to American Board of Radiology (ABR) Maintenance of Certificate (MOC) for Prof. Dr. Axel Wismüller. Prof. Dr. Dr. Maximilian Reiser, FACR, FRCR of the Department of Radiology, Ludwig Maximilian University Munich, Germany, is also acknowledged for his continued support.

References

1. Lang TF, Keyak JH, Heitz MW, Augat P, Lu Y, Mathur A, Genant HK. Volumetric quantitative computed tomography of the proximal femur: precision and relation to bone strength. Bone. 1997; 21(1):101–108. [PubMed: 9213015]
2. Bauer JS, Link TM. Advances in osteoporosis imaging. European Journal of Radiology. 2009; 71(3):440–449. [PubMed: 19651482]
3. Bauer JS, Kohlmann S, Eckstein F, Mueller D, Lochmüller EM, Link TM. Structural analysis of trabecular bone of the proximal femur using multi-slice computed tomography: a comparison with dual x-ray absorptiometry for predicting biomechanical strength in vitro. Calcified Tissue International. 2006; 78(2):78–89. [PubMed: 16467973]
4. Baum T, Carballido-Gamio J, Huber MB, Mueller D, Monetti R, Räth C, Eckstein F, Lochmüller EM, Majumdar S, Rummeny E, Link TM, Bauer JS. Automated 3D trabecular bone structure analysis of the proximal femur prediction of biomechanical strength by CT and DXA. Osteoporosis International. 2010; 21:1553–1564. [PubMed: 19859642]
5. Yang CC, Nagarajan MB, Huber MB, Carballido-Gamio J, Bauer JS, Baum T, Eckstein F, Lochmüller E, Majumdar S, Link TM, Wismüller A. Improving bone strength prediction in human proximal femur specimens through geometrical characterization of trabecular bone microarchitecture and support vector regression. Journal of Electronic Imaging. Jan-Feb;2014
6. Huber MB, Carballido-Gamio J, Bauer JS, Baum T, Eckstein F, Lochmüller EM, Majumdar S, Link TM. Proximal femur specimens: automated 3D trabecular bone mineral density analysis at multi-

detector CT-correlation with biomechanical strength measurement. Radiology. 2008; 247:472–481. [PubMed: 18430879]

7. Baum T, Gräbeldinger M, Räth C, Garcia EG, Burgkart R, Patsch JM, Rummeny EJ, Link TM, Bauer JS. Trabecular bone structure analysis of the spine using clinical MDCT: can it predict vertebral bone strength? JBMM. Apr 20.2013
8. Jamitzky F, Starka RW, Bunkb W, Thalhammera S, Räth C, Aschenbrennerb T, Morfill GE, Heckla WM. Scaling-index method as an image processing tool in scanning-probe microscopy. Ultramicroscopy. 2001; 86:241–246. [PubMed: 11215629]
9. Hoole P, Wismüller A, Leinsinger G, Kroos C, Geumann A, Inoue M. Analysis of tongue configuration in multi-speaker, multi-volume MRI data. Proc 5th Semin Speech Prod Model Data CREST Work Model Speech Prod Mot Plan Articul Model. 2000:157–160.
10. Wismüller, A. Ph.D. Thesis. Technical University of Munich, Department of Electrical and Computer Engineering; 2006. Exploratory Morphogenesis (XOM): a novel computational framework for self-organization.
11. Wismüller, A., Dersch, DR., Lipinski, B., Hahn, K., Auer, D. ICANN 98. Springer; London: 1998. A neural network approach to functional MRI pattern analysis—clustering of time-series by hierarchical vector quantization; p. 857-862.
12. Wismüller, A., Vietze, F., Dersch, DR., Behrends, J., Hahn, K., Ritter, H. Neurocomputing. Vol. 48. Elsevier; 2002. The deformable feature map-a novel neurocomputing algorithm for adaptive plasticity in pattern analysis; p. 107-139.
13. Behrends, J., Hoole, P., Leinsinger, GL., Tillmann, HG., Hahn, K., Reiser, M., Wismüller, A. Bildverarbeitung für die Medizin 2003. Springer; Berlin, Heidelberg: 2003. A segmentation and analysis method for MRI data of the human vocal tract; p. 186-190.
14. Wismüller A, Dersch DR. Neural network computation in biomedical research: chances for conceptual cross-fertilization. Theory in Biosciences. 1997; 116(3):229–240.
15. Bunte K, Hammer B, Villmann T, Biehl M, Wismüller A. Exploratory Observation Machine (XOM) with Kullback-Leibler Divergence for Dimensionality Reduction and Visualization. ESANN. 2010; 10:87–92.
16. Wismüller, A., Vietze, F., Dersch, DR., Hahn, K., Ritter, H. ICANN 98. Springer; London: 1998. The deformable feature map—adaptive plasticity for function approximation; p. 123-128.
17. Wismüller, A. Advances in Self-Organizing Maps. Springer; Berlin Heidelberg: 2009. The exploration machine–a novel method for data visualization; p. 344-352.
18. Wismüller, A. Method, data processing device and computer program product for processing data. US Patent. 7,567,889. 2009.
19. Meyer-Bäse, A., Jancke, K., Wismüller, A., Foo, S., Martinetz, T. Eng Appl Artif Intell. Vol. 18. Elsevier; 2005. Medical image compression using topology-preserving neural networks; p. 383-392.
20. Huber, MB., Nagarajan, M., Leinsinger, G., Ray, LA., Wismüller, A. SPIE Med Imaging 7624, 762410. International Society for Optics and Photonics; 2010. Classification of interstitial lung disease patterns with topological texture features.
21. Wismüller A. The exploration machine: a novel method for analyzing high-dimensional data in computer-aided diagnosis. SPIE Med Imaging, 72600G – 72600G. 2009
22. Bunte, K., Hammer, B., Villmann, T., Biehl, M., Wismüller, A. Neurocomputing. Vol. 74. Elsevier; 2011. Neighbor embedding XOM for dimension reduction and visualization; p. 1340-1350.
23. Wismüller, A. Advances in Self-Organizing Maps. Springer; Berlin Heidelberg: 2009. A computational framework for nonlinear dimensionality reduction and clustering; p. 334-343.
24. Huber, MB., Nagarajan, MB., Leinsinger, G., Eibel, R., Ray, LA., Wismüller, A. Med Phys. Vol. 38. American Association of Physicists in Medicine; 2011. Performance of topological texture features to classify fibrotic interstitial lung disease patterns; p. 2035-2044.
25. Wismüller A, Verleysen M, Aupetit M, Lee JA. Recent Advances in Nonlinear Dimensionality Reduction, Manifold and Topological Learning. ESANN. 2010
26. Wismüller, A., Meyer-Baese, A., Lange, O., Reiser, MF., Leinsinger, G. Med Imaging, IEEE Trans. Vol. 25. IEEE; 2006. Cluster analysis of dynamic cerebral contrast-enhanced perfusion MRI time-series; p. 62-73.

27. Otto TD, Meyer-Bäse A, Hurdal M, Sumners D, Auer D, Wismüller A. Model-free functional MRI analysis using cluster-based methods. AeroSense. 2003; 2003:17–24.
28. Varini C, Nattkemper TW, Degenhard A, Wismüller A. Breast MRI data analysis by LLE. Neural Networks, 2004. Proceedings. 2004 IEEE Int Jt Conf. 2004; 3:2449–2454.
29. Huber, MB., Lancianese, SL., Nagarajan, MB., Ikpot, IZ., Lerner, AL., Wismüller, A. Biomed Eng IEEE Trans. Vol. 58. IEEE; 2011. Prediction of biomechanical properties of trabecular bone in MR images with geometric features and support vector regression; p. 1820-1826.
30. Meyer-Base A, Pilyugin SS, Wismüller A. Stability analysis of a self-organizing neural network with feedforward and feedback dynamics. Neural Networks, 2004. Proceedings. 2004 IEEE Int Jt Conf. 2004; 2:1505–1509.
31. Wismüller, A., Meyer-Bäse, A., Lange, O., Schlossbauer, T., Kallergi, M., Reiser, MF., Leinsinger, G. J Electron Imaging. Vol. 15. International Society for Optics and Photonics; 2006. Segmentation and classification of dynamic breast magnetic resonance image data; p. 13020-013020-13.
32. Nagarajan, MB., Huber, MB., Schlossbauer, T., Leinsinger, G., Krol, A., Wismüller, A. Mach Vis Appl. Vol. 24. Springer; Berlin Heidelberg: 2013. Classification of small lesions in dynamic breast MRI: eliminating the need for precise lesion segmentation through spatio-temporal analysis of contrast enhancement; p. 1371-1381.
33. Nagarajan, MB., Huber, MB., Schlossbauer, T., Leinsinger, G., Krol, A., Wismüller, A. J Med Biol Eng. Vol. 33. NIH Public Access; 2013. Classification of Small Lesions in Breast MRI: Evaluating The Role of Dynamically Extracted Texture Features Through Feature Selection.

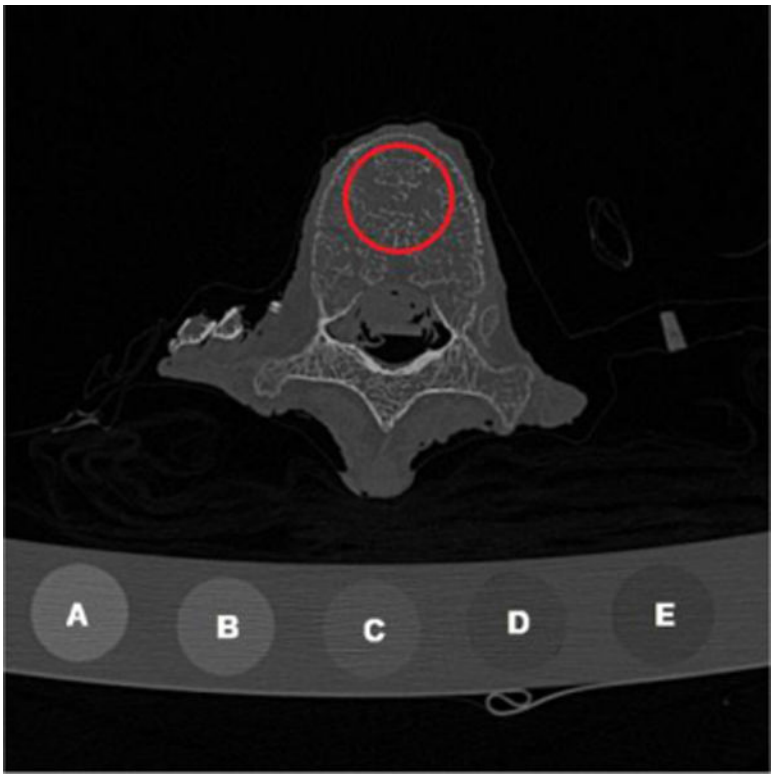

Figure 1.

The central axial slice from the middle vertebra. The calibration phantoms A-E are seen on the bottom; their equivalent H_20 and K_2HPO_4 densities are specified in [4]. A 2D representation of a sample VOI selected for analysis of trabecular bone structure is outlined in red. The phantom portions A and E are used as equivalent bone and water phantoms respectively in line with [7].

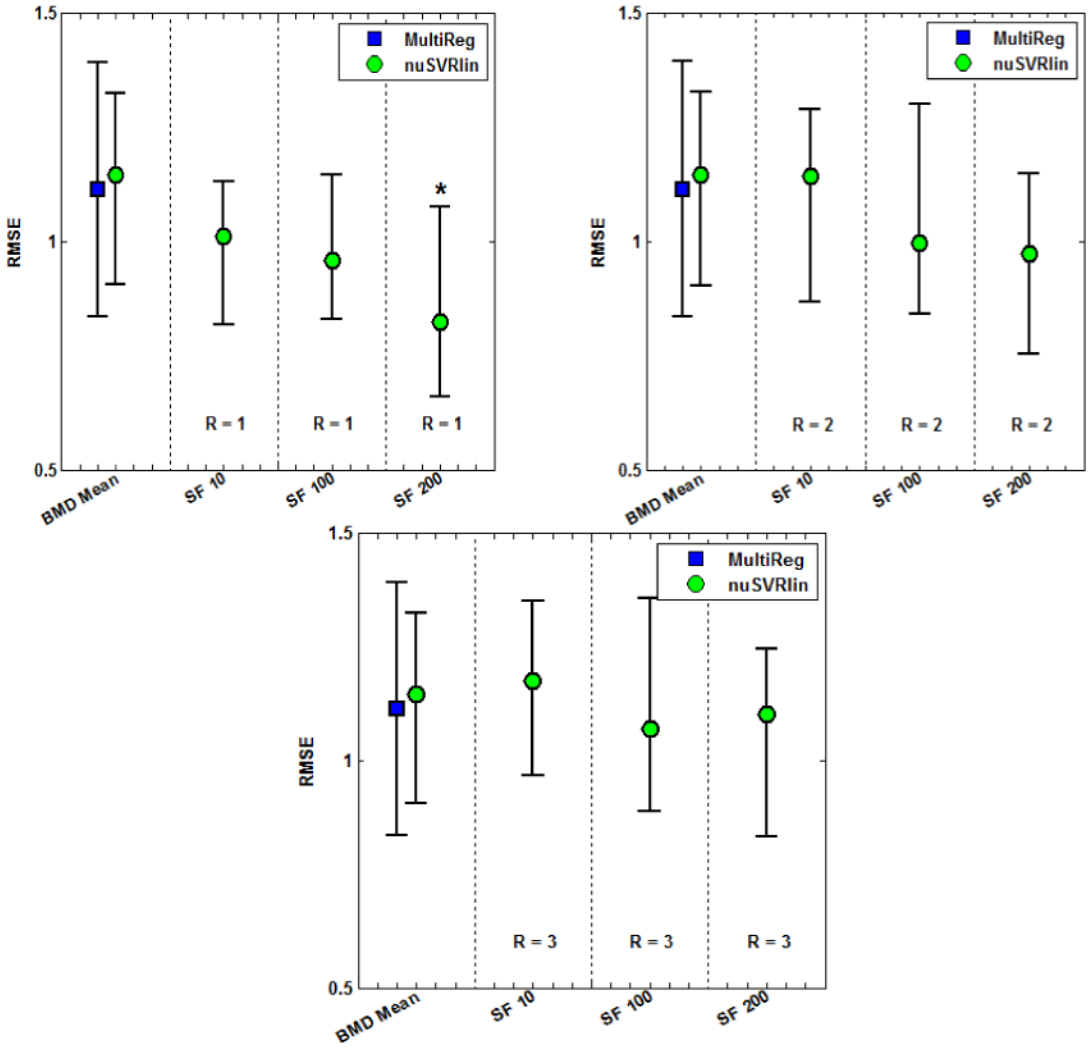

Figure 2.

Prediction performance plotted for different scaling factors (SFs) for a radius R of 1, 2 and 3 compared to the BMD mean (first column in blue); MultiReg – multiple regression, nuSVRlin – support vector machine with linear kernel. For each RMSE distribution, the central mark corresponds to the median and the edges are the 25th and 75th percentile. Multiple regression results for high dimensional SIM features cannot be represented in the graphs, as the RMSE values are higher than 1.5. Statistically significant results can be seen for an R = 1 and SF = 200 when using nuSVRlin.